Hrvatski meteorološki časopis, 26, Zagreb, 1991, str. 19-40

UDK: 551.555.4
Originalni znanstveni rad

Application of the Hydraulic Theory to Naturally Occurring Bora Flow

Primjena hidrauličke teorije na prirodni tok bure

Vesna Jurčec and Dražen Glasnović

Republički hidrometeorološki zavod, Zagreb, Hrvatska
Primljeno 01.07. 1991, u konačnom obliku 09.08. 1991

Abstract

This paper deals with the application of Smith's (1985) internal hydraulic theory to some special cases of Adriatic bora during ALPEX SOP. In particular, the case of 15 April 1982 is analysed for which the numerical simulation by Klemp and Durran (1987) is available. Their conclusion is that in this case neither inversion nor critical level are important for the bora occurrence, but the low-level wave breaking due to weak flow in the upstream region. While this conclusion seems reasonable, from the present analysis it is argued that these results are valid only for the characteristics of the local bora in Senj and not for the flow across the higher mountains along the northern Adriatic coast.

This conclusion is based on a comparison with the results of the theory application to the stronger bora condition on the previous day and especially to the case of the strongest SOP bora on 6 March 1982 for which the hydraulic theory offered much better results.

Key words: Adriatic bora, hydraulic flow, wave breaking, severe winds.

Sažetak

Analizirani su rezultati primjene hidrauličke teorije Smitha (1985) na neke slučajeve bure na Jadranu za vrijeme specijalnog perioda osmatranja Alpskog eksperimenta (ALPEX SOP). Posebno je prikazan slučaj bure od 15. travnja 1982, za koji postoje rezultati numeričke simulacije Klempa i Durrana (1987). Njihov je zaključak da u ovom slučaju za pojavu bure nisu važni inverzija temperature ili kritični nivo, nego lom vala u niskoj troposferi uzrokovan slabim strujanjem u navjetrini planine. Iako je iz prikazane analize ovaj zaključak prihvatljiv naglašava se da ti rezultati vrijede samo za karakteristike lokalne bure u Senju, a ne za tok preko viših planina duž ostalog dijela obale sjevernog Jadrana.

Ovaj je zaključak izveden i iz usporedbe s primjenom teorije u situaciji s jačom burom prethodnog dana, a posebno za slučaj s najjačom burom u SOP od 6. ožujka 1982. za koji je hidraulička teorija dala mnogo bolje rezultate.

Ključne riječi: Bura na Jadranu, hidraulički tok, lom vala, olujni vjetar.

1. Introduction

Bora was traditionally viewed as a fall wind consisting of a cold airstream accelerating as it moves downstream due to its high density and gravity force. Smith (1987) drew attention to the hydraulic mechanism for the bora. Hydraulics refers to hydrostatic flow with a constant pressure condition applied to an upper streamline. The role of the wind reversal aloft, or a significant inversion capping the bora layer with NE cold air stream, is a decoupling of the upper and lower regions which prevents the disturbance aloft. The upper fluid then imposes no pressure gradient on the lower fluid which in such case accelerates according to hydraulic laws.

Mountain wave simulation by Clark and Peltier (1977) have shown that a forced internal wave reaching a very large amplitude may exceed critical steepness and "break" in such a way that streamlines locally overturn. This then triggers a new process leading to a large increase in wave amplitude at low levels. The level of breaking becomes the "wave-induced critical level" leading to wave reflection which may interfere with the incident wave so that the wave-field at low levels may amplify resonantly. According to this theory, breaking is essential for understanding the behaviour of severe downslope winds and the resonant amplification process is fundamental to the dynamics of the naturally occurring flow which bears a strong qualitative resemblance to the characteristics associated with hydraulic jumps.

Smith (1985) proposed an alternative description of the wave-breaking amplification process assuming that the breaking region traps the wave energy within the underlying flow and forms a stagnant overturned "dead" layer with constant temperature and negligible pressure perturbation aloft. Thus, the wave overturning region appears in both Smith's and Clark-Peltier's theories as a localized critical layer with a small Ri-number, and of limited horizontal extent.

Durran and Klemp (1987) have shown that when the height of the critical level H_0 is smaller than the vertical wavelength L_Z the stratified flow beneath H_0 exhibits a pronounced similarity to the hydraulic system described by the shallow water theory. However, when $H_0 > L_Z$ internal perturbations appear in the flow which are not present in the shallow system.

According to the Peltier-Clark's (1983) linear resonance amplification mechanism severe states should develop only when the height of the critical layer is 1/4, 3/4, 5/4, ... vertical wavelengths above the ground. Their vertical wavelength calculation was based on the constant values of stability and wind below the critical layer. The results predict large amplitude responses at the critical levels of 0.75 L_Z and 1.25 L_Z, which was not confirmed in Durran and Klemp's results. Clark and Peltier, however, presented no experiments below 0.75 L_Z, in the very region where Durran and Klemp found the greatest conflict between their results and the resonance hypothesis.

On the other hand Smith's solution of the displacement of the dividing streamline from its undisturbed position shows that with a sufficiently high mountain this displacement would reach the turning point where $\partial\hat{h}/\partial\hat{\delta} = 0$ and the flow could transition to a new regime in which the lower part of the dividing streamline would continuously descend along the lee slope. As the initial height of the dividing streamline increases, $\hat{h}$ required to produce the transition also increases. The solution technique fails when $\hat{h}$ becomes greater than that required to produce transition.

Long's equation for an atmosphere with constant mean wind and stability (no critical layer) indicates that wave-breaking will occur at the level 0.75 L_Z when effective mountain height, $\hat{h}_m$, exceeds 0.85. Thus, if $\hat{h}$ is sufficiently high and the elevation of the mean-flow critical layer exceeds 0.75 L_Z wave breaking may still develop beneath the mean-flow critical layer, producing a strong response.

To conclude, Durran and Klemp have shown that the response of the simulated flow to changes in the critical-layer height

and the mountain height is in good agreement with Smith's theory suggesting that the strong downslope winds associated with wave-overturning are caused by continuously stratified analog to the transition from subcritical to supercritical flow in the conventional hydraulic theory of shallow water.

Our study is first concern with the results of the numerical simulation of bora wind by Klemp and Durran (1987) in which they analysed the structure of the bora flow using aircraft observations collected during the ALPEX SOP on 15 April 1982. Using the upstream sounding data from Zagreb and varying the environmental sounding in the simulations they found that in *this case neither the critical layer nor the inversion play a fundamental dynamical role in generating strong bora wind. The most important factor* is *the overturning of the wave beneath the inversion and critical level.* The low-level flow structure was significantly altered in the experiment when an inversion or critical layer was located beneath the overturning layer. Klemp and Durran's experiments have shown that even in the investigated case it was likely that *the pool of cold air in the upstream region was largely responsible for producing the cross-mountain flow beneath the inversion.*

The essential result of these experiments is that it is the role of internal stratification, not the rapid change of temperature across the inversion, which is primarily responsible for bora generation. It is considered that *the process of overturning and breaking is likely to dominate the dynamics of bora flow whenever the cross-mountain flow is weak.* In this case $\hat{h} = h\ N/U$ is large, indicating that the wave amplitude is sufficient to produce breaking. At the same time the vertical wavelength $L_Z = 2\ \pi\ U/N$ is small and there is an increasing chance of a wave breaking level forming below the inversion and the critical level. When the parameter $\hat{h}$ is smaller than the value required to produce overturning or when the inversion is below the level at which overturning would occur, the wave structure may be governed by hydraulic flow dynamics. To conclude, the simulation results by Klemp and Durran suggest that the shooting flows produced by the hydraulic theory may be fundamentally similar to those produced by wave breaking.

It is the purpose of this study to present more details of the bora structure and behaviour on the day of 15 April 1982 in comparison to the bora occurrence on the previous day with stronger wind, and the two-day period 6-7 March 1982 with the strongest SOP bora case and its rapid decay. The presentation will follow an earlier work by the authors (Glasnović and Jurčec, 1990) with particular emphasis on the application of Smith's (1985) hydraulic theory of severe downslope winds indicating the problem of solution technique when applied to the bora cases like the one on 15 April 1982.

2. Characteristics of the Case Studies

Detailed description of the case study of 14-15 April is presented by Vučetić (1989) and the one of 6-7 March by Bajić (1989). Fig. 1 shows the daily course of bora wind speed for these two cases in Senj and Omišalj (the island of Krk). This illustrates the persistency of bora in Senj, and it clearly shows that bora at this locality is not representative of the larger area of the northern Adriatic, not even of Omišalj which is relatively close to Senj.

The local characteristics of the bora course are very similar in the two cases considered in Fig. 1, indicating that on the first day Omišalj reaches the same, or higher, wind speed whereas on the second day bora rapidly decreases in this locality under the conditions which obviously do not influence the famous bora in Senj.

Thus, the environmental condition represented by the Zagreb sounding on 15 April used for the bora simulation by Klemp and Durran, and the aerial observations carried out by research flights in SOP on this day indicated favourable weather conditions for the bora in Senj but not for the bora along the entire northern Adriatic coast.

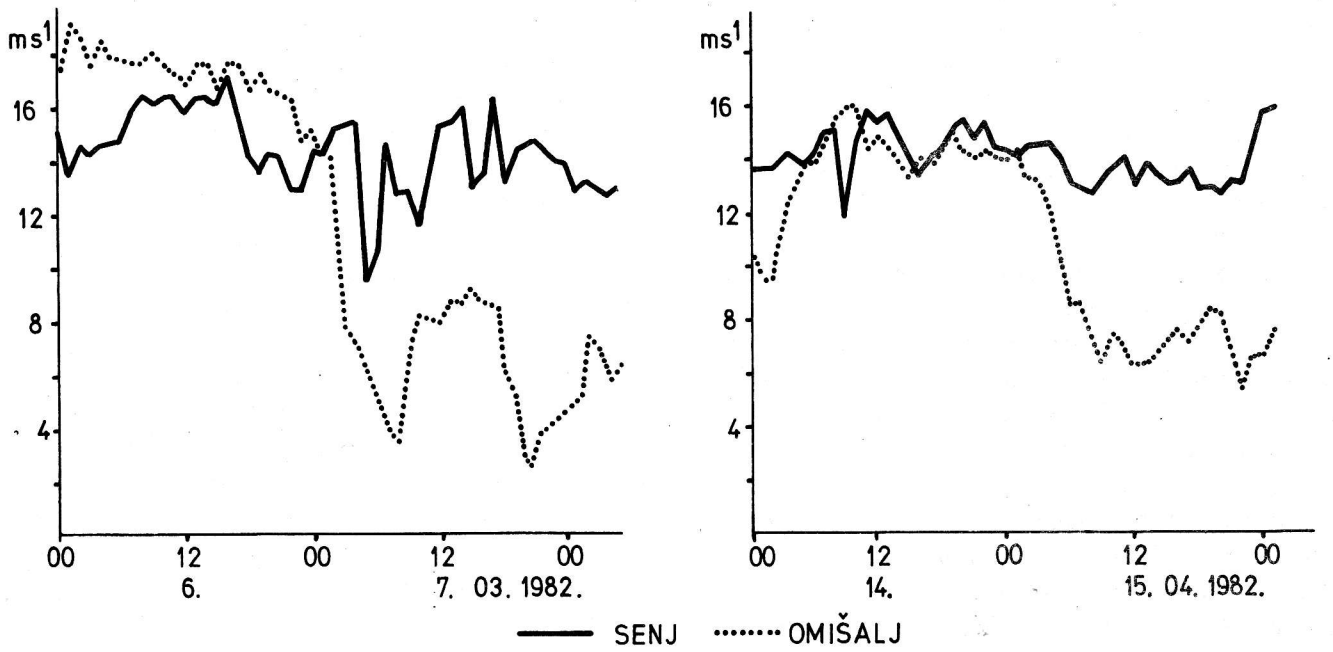

Fig. 1 Daily courses of bora wind for Senj and Omišalj 6-7 March and 14-15 April 1982.
Sl. 1 Dnevni hod bure za Senj i Omišalj za 6-7 ožujak i 14-15 travanj 1982.

Figs. 2.1 - 2.9 present the vertical profiles of temperature, wind speed and direction, stability in the form of Brunt-Väisälä frequency, Scorer parameter and the profile of vertical acceleration. All of these quantities have been studied by Glasnović (1983) in an isentropic coordinate system and also discussed by Glasnović (1990) and Glasnović and Jurčec (1990) for some of the bora cases, and this is only a brief review.

Static stability is calculated as the reciprocal value of the thermal stability parameter in which the nonhydrostatic coefficient E_a is defined by

$$E_a = 1 + \partial \ln\varepsilon / \partial \ln\Theta \qquad (1)$$

Under hydrostatic approximation it is equal to zero so that

$$\frac{\partial p}{\partial \Theta} = \frac{1}{\varkappa} \frac{p}{\varepsilon} \frac{\partial \varepsilon}{\partial \Theta} \text{ or } \frac{\partial p}{\partial \Theta} = - \frac{1}{\varkappa} \frac{p}{\Theta} \qquad (2)$$

Since the derivative of Exner function $\varepsilon = c_p (p/p_0)^{\varkappa}$ valid under hydrostatic assumption in the isentropic coordinate system is $\partial\varepsilon/\partial\Theta = - \varepsilon/\Theta$.

From the expression of static stability defined by

$$S = \frac{g}{T} \Gamma_d (1+E_a) \qquad (3)$$

where $\Gamma_d = g/c_p$ is the dry adiabatic lapse rate, vertical acceleration is expressed by its original relation

$$dw/dt = - S \Delta z \qquad (4)$$

In a stable state, when $-1 < E_a < 1$, $S > 0$, $dw/dt < 0$ indicates an intensification of descending motion or ascending motion retardation.

Fig. 2.1 shows these parameters for Zagreb on 15 April 1982, 00 UTC. The most characteristic feature is the temperature inversion which occurs simultaneously with a wind decrease at an altitude between 2 and 3 km, where the wind direction rapidly changes from NE to S-SW. The low-level speed profile shows a maximum value of 11 ms^{-1} with a sharp wind shear below and above this peak. This is clearly seen in a graph of the Scorer parameter,

$$\ell = N/U \qquad (5)$$

which indicates the ratio of the Brunt-Väisälä frequency and the wind speed. Thus,

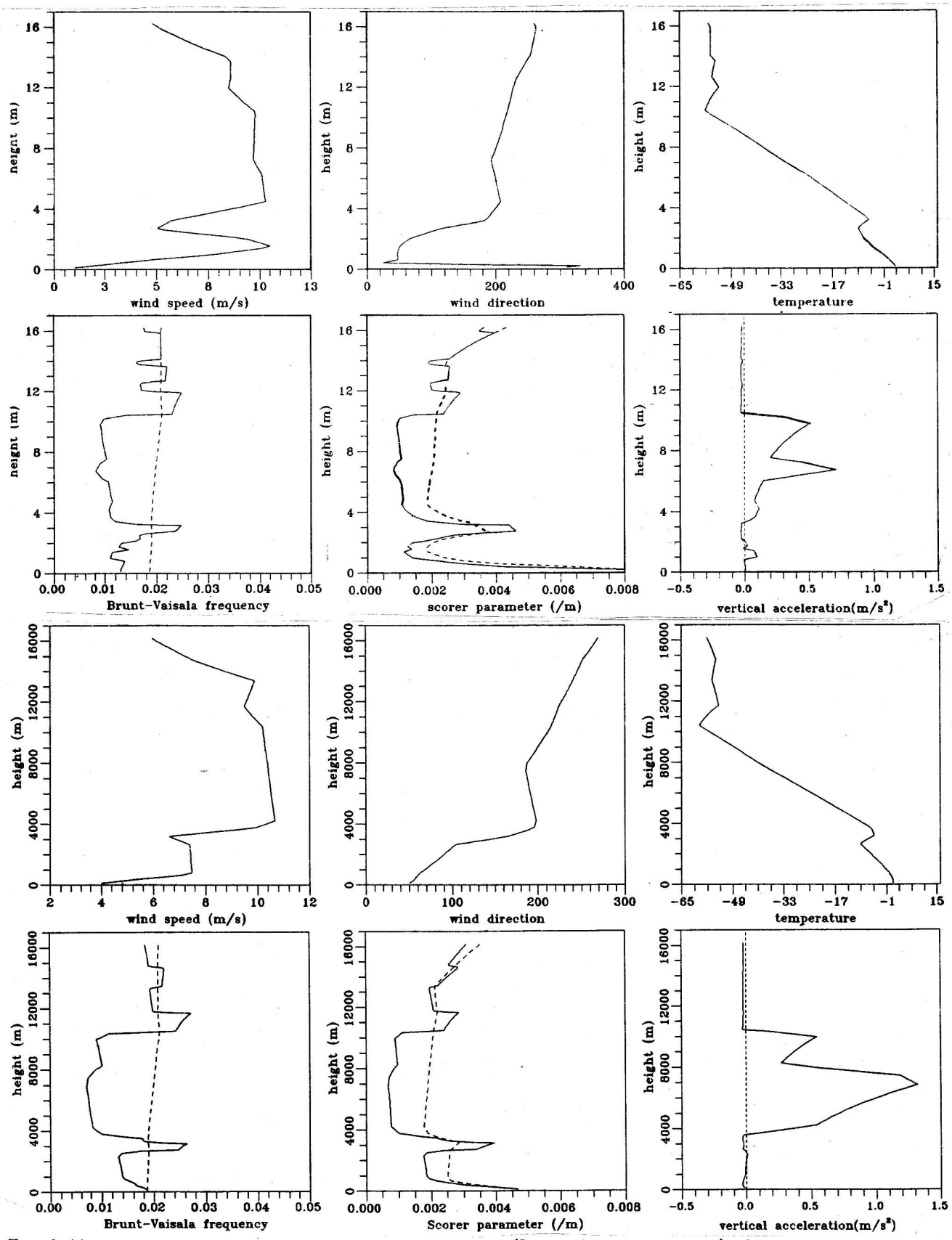

Fig. 2 Vertical profiles of wind and temperature, stability (Brunt Väisälä frequency), Scorer parameter ℓ=N/U and vertical acceleration (Eq. 4) for indicated days in the period 6-7 March and 14-15 April 1982, for Zagreb, Karlovac and Pula.

Sl. 2 Vertikalni profili vjetra i temperature, stabilnosti (Brunt-Väisälä frekvencije), Scorerovog parametra, ℓ=N/U, i vertikalne akceleracije (jedn. 4) za označene dane u razdoblju 6-7 ožujak i 14-15 travanj 1982, za Zagreb, Karlovac i Pulu.

Fig. 2.1 Zagreb, 15 April 1982, 00 UTC (above)
Sl. 2.1 Zagreb, 15 travanj 1982, 00 UTC (gore)

Fig. 2.2 Karlovac, 15 April 1982, 00 UTC (below)
Sl. 2.2 Karlovac, 15 travanj 1982, 00 UTC (dolje)

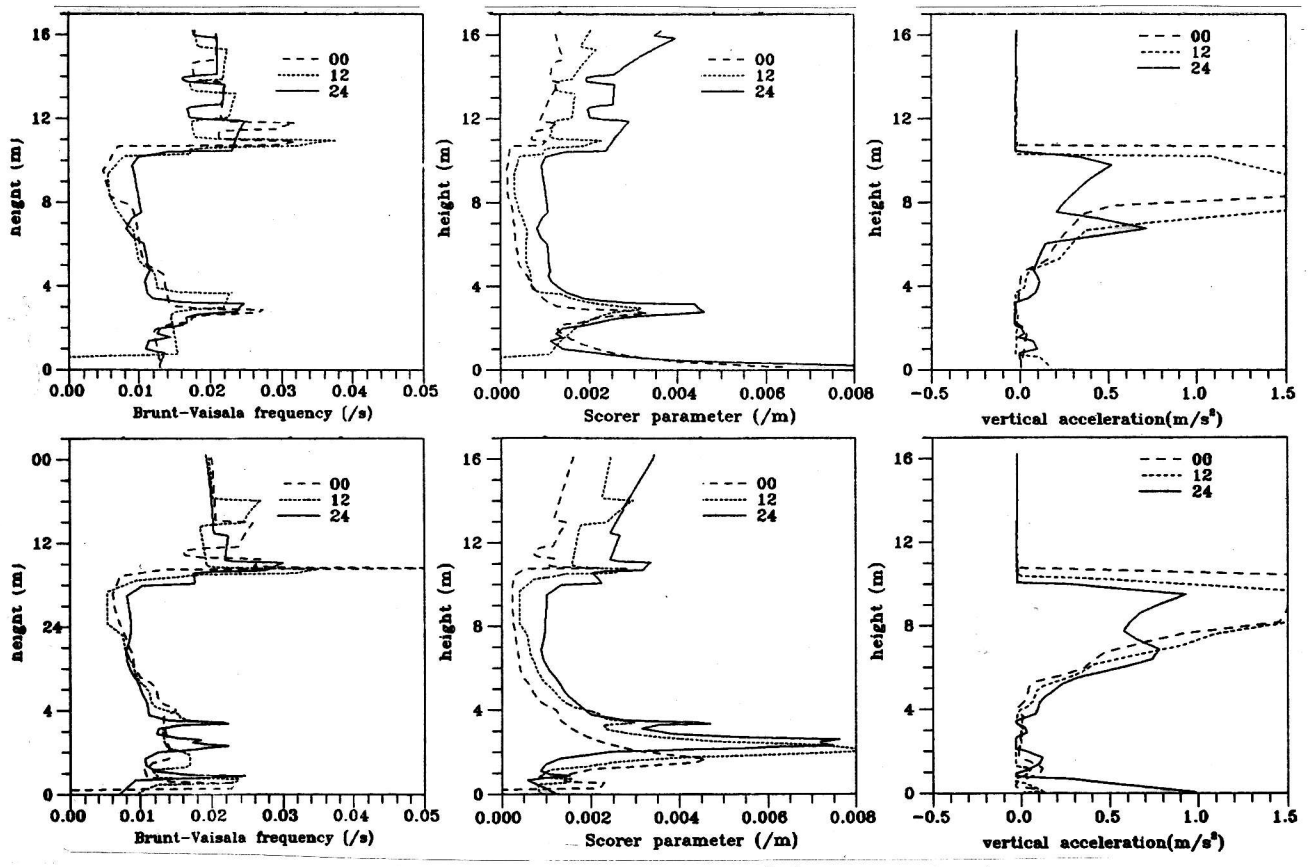

Fig. 2.3 Zagreb and Pula, 14 April 1982, 00 + 12 + 24 UTC (12-hourly intervals).
Sl. 2.3 Zagreb i Pula, 14 travanj 1982, 00 + 12 + 24 UTC (12-satni intervali)

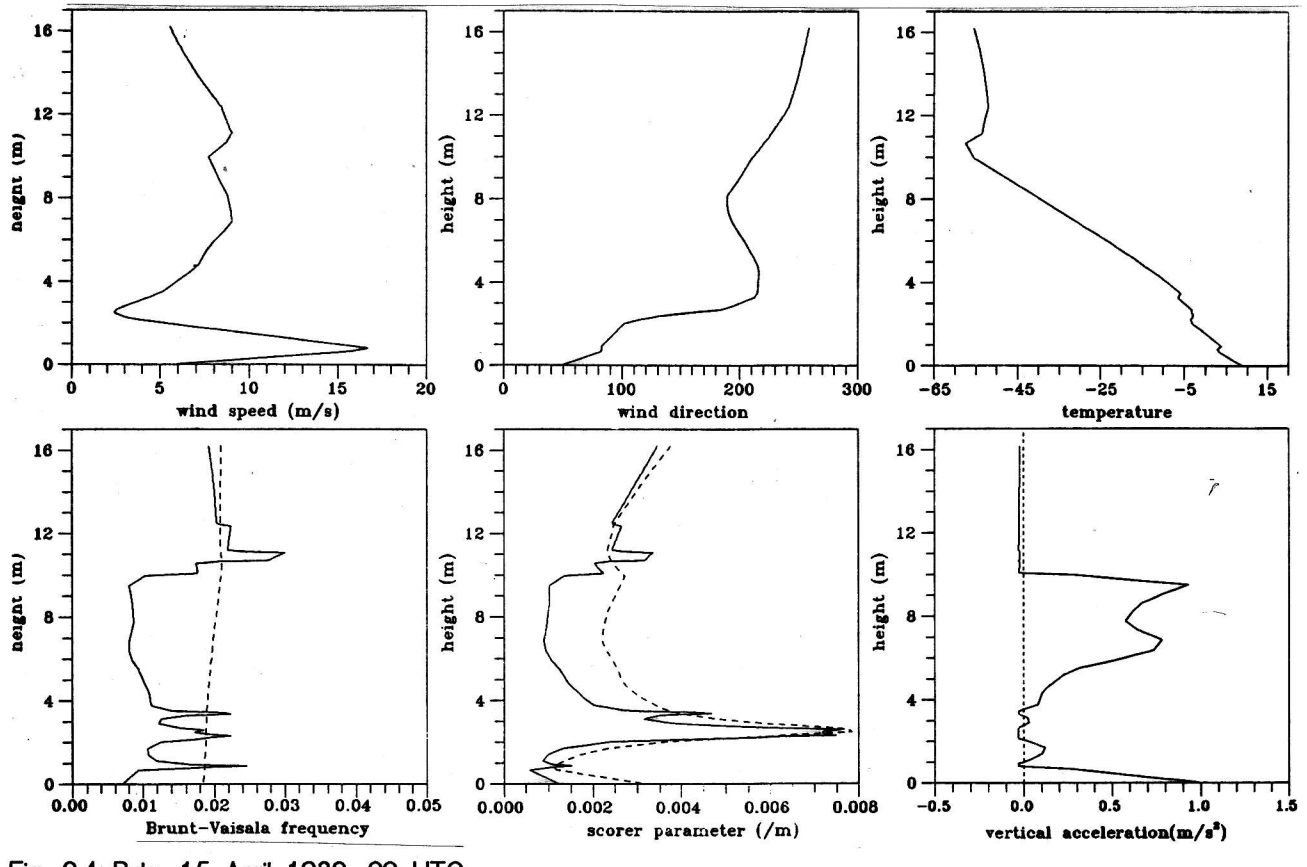

Fig. 2.4 Pula, 15 April 1982, 00 UTC
Sl. 2.4 Pula, 15 travanj 1982, 00 UTC

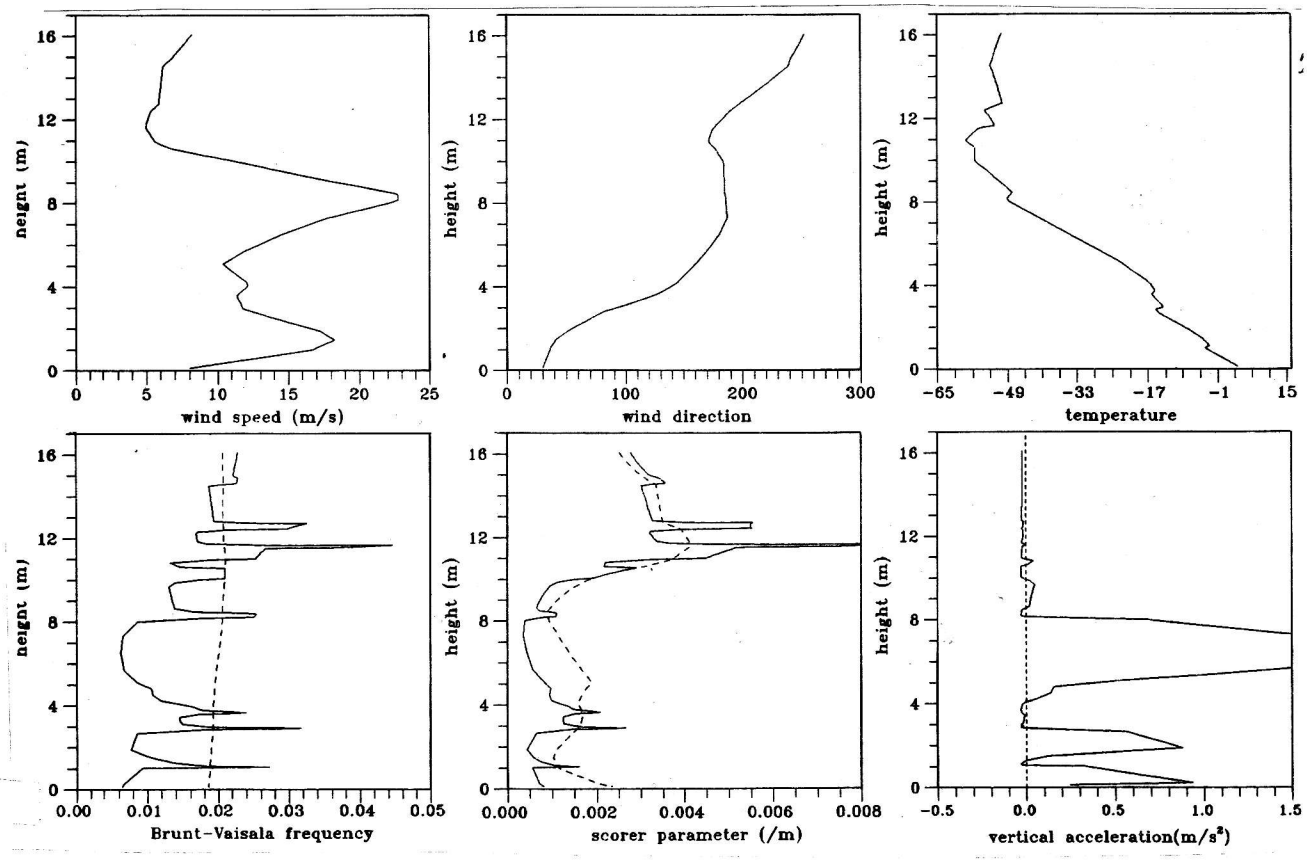

Fig. 2.5 Zagreb, 6 March 1982, 06 UTC
Sl. 2.5 Zagreb, 6 ožujak 1982, 06 UTC

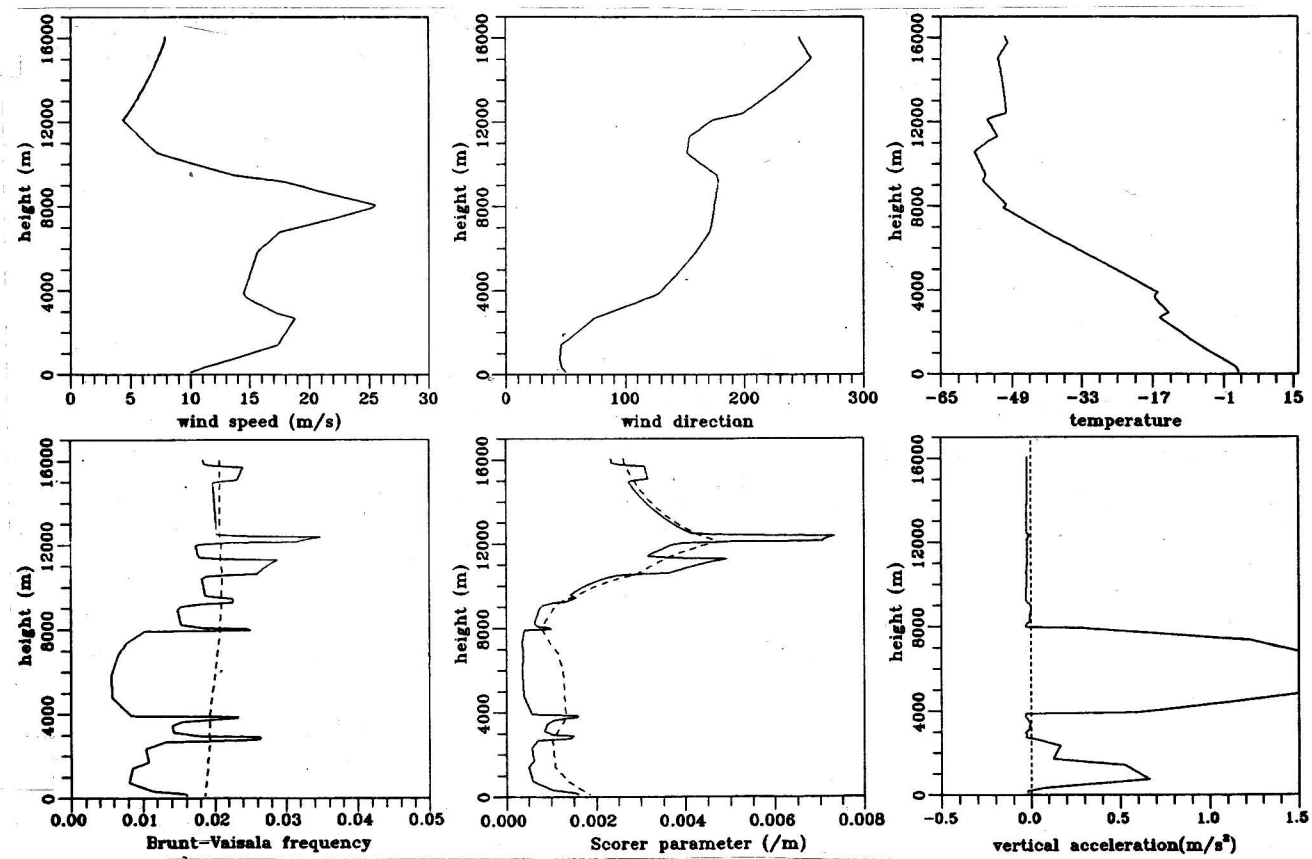

Fig. 2.6 Karlovac, 6 March 1982 06 UTC
Sl. 2.6 Karlovac, 6 ožujak 1982, 06 UTC

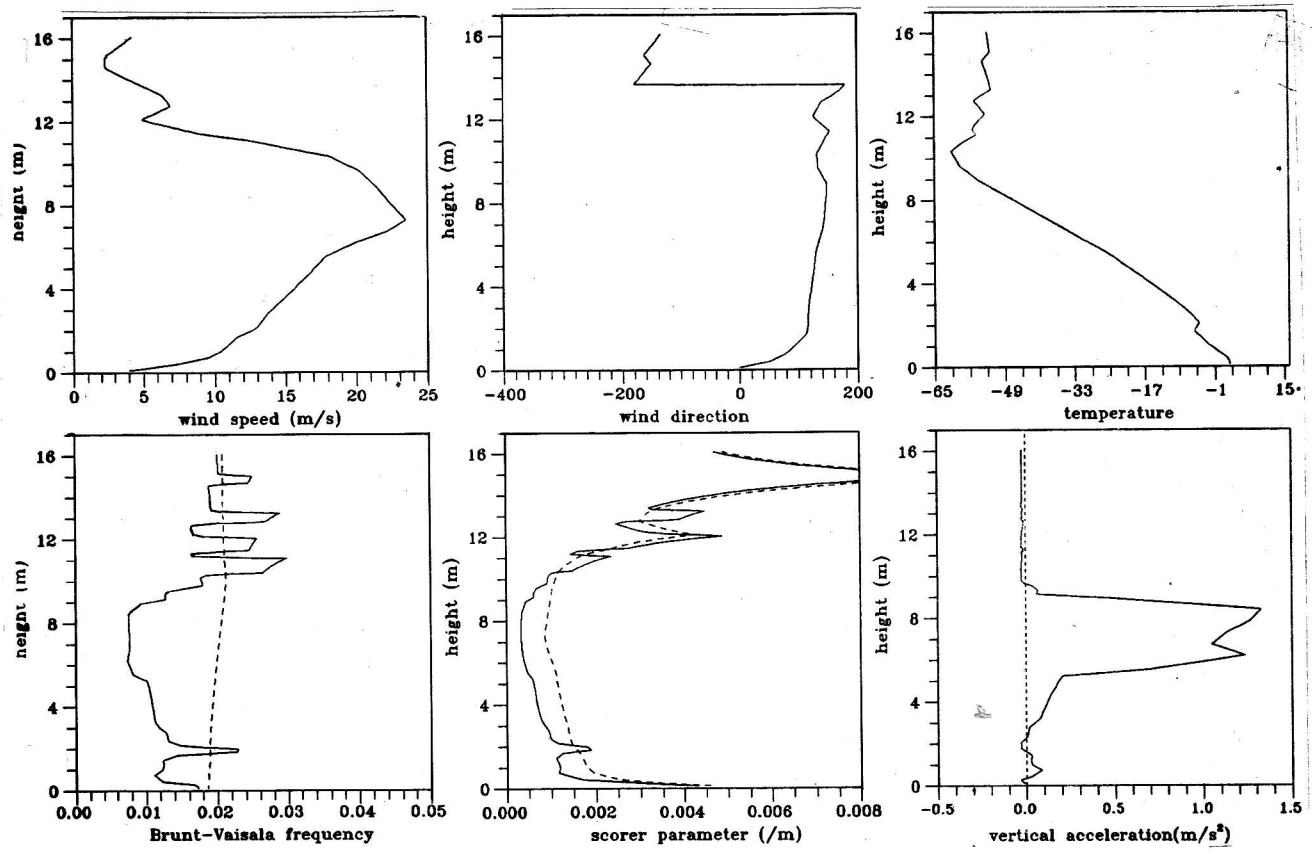

Fig. 2.7 Zagreb, 7 March 1982, 18 UTC
Sl. 2.7 Zagreb, 7 ožujak 1982, 18 UTC

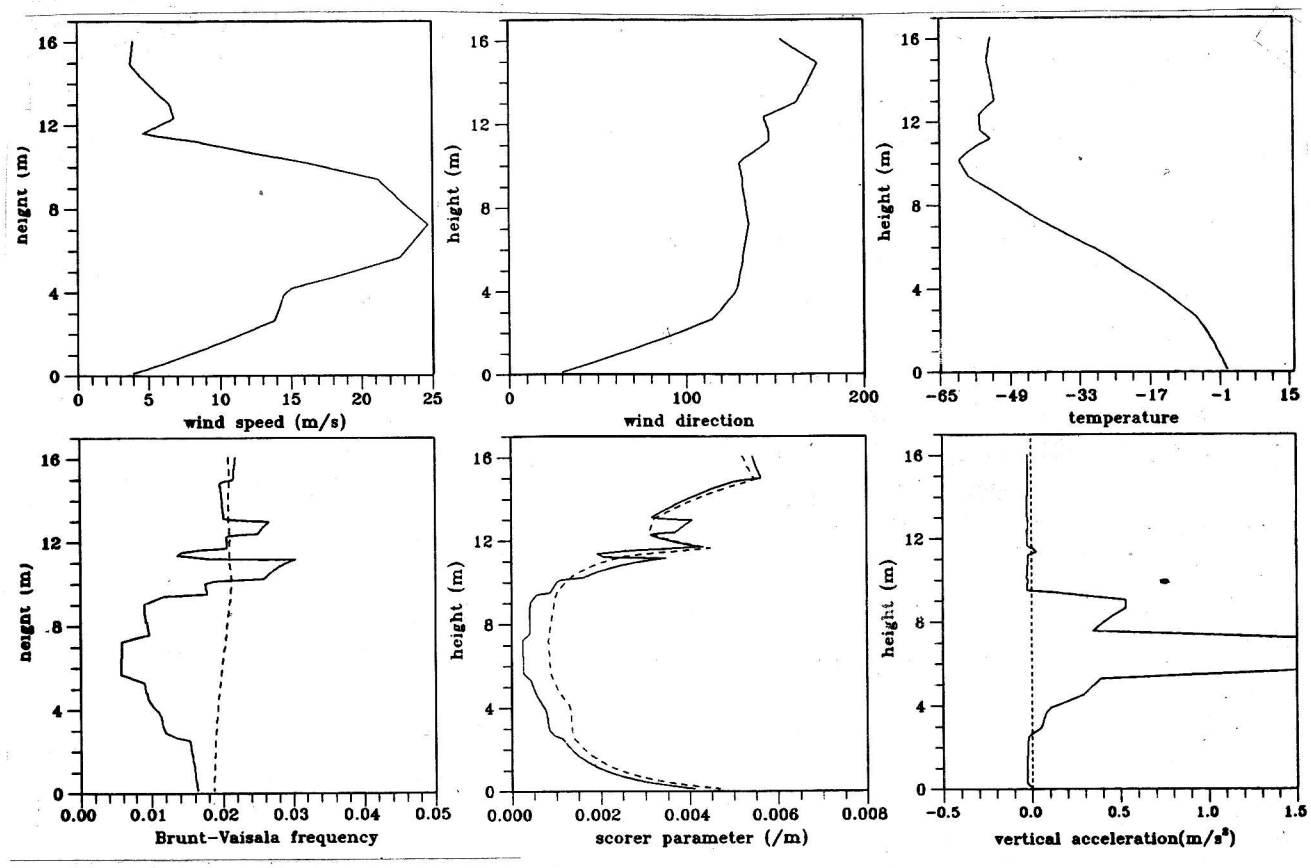

Fig. 2.8 Karlovac, 7 March 1982, 18 UTC
Sl. 2.8 Karlovac, 7 ožujak, 1982, 18 UTC

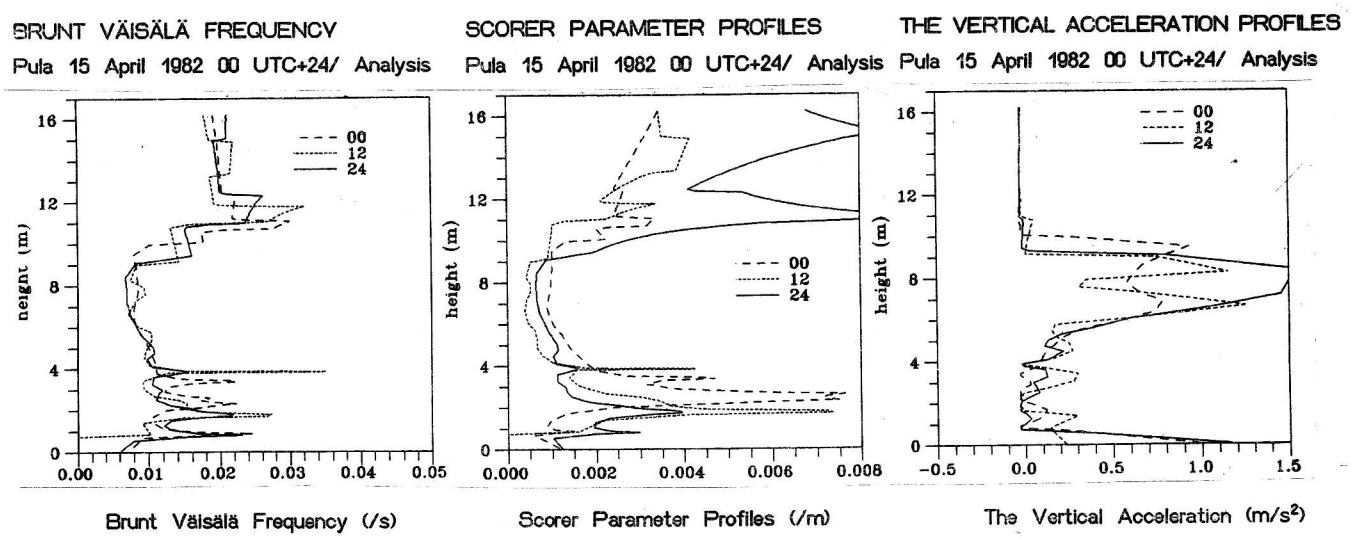

Fig. 2.9 Pula, 6 March 1982, 00 + 12 + 24 UTC
Sl. 2.9 Pula, 6 ožujak 1982, 00 + 12 + 24 UTC

the pronounced maxima of Scorer parameter are the result of both stability and wind decrease. A smaller maximum of ℓ, shown by a dashed curve results from the hydrostatic stability calculated from (2) which is also shown in the stability graph. This graph shows that hydrostatic stability is generally higher than the actual and it is constant in the bora layer as required by the model. On the other hand for this very reason it can not detect temperature inversion capping the bora layer, which therefore needs to be presented by the actual temperature profile. How representative are the temperature and wind profiles shown in Fig. 2.1 for the upstream bora region? Fig. 2.2 presents the graphs of the same vertical profiles for Karlovac placed about 50 km to the south of Zagreb. It is seen that the basic features found in Zagreb were also observed at this location except for a weaker low-level wind maximum.

The vertical profile of vertical acceleration has a common feature in both figures - a sharp increase in this parameter below the tropopause. However, in this particular case there are two maxima in the upper troposphere and a smaller increase in this parameter in the low tropospheric structure of Zagreb. This feature is more pronounced in the profile of Pula in Fig. 2.4.

To illustrate the differences in the wind and temperature structure on the previous day with stronger bora, Fig. 2.3 shows stability and Scorer parameter superimposed at 12-hourly intervals for Zagreb which stresses the persistency of the inversion level.

The last graphs illustrating this case, given in Fig. 2.4, are the profiles for Pula on 15 April, 00 UTC. It is seen that temperature structure is rather complex, with three inversions in the lower troposphere, and that the wind maximum appears above the ground in a very shallow bora layer. Thus, at this particular locality surface wind is not very strong, but it rapidly increases with height in this shallow layer, i.e. the maximum bora component does not

reach the ground in this period.

Fig. 2.5 and 2.6 show the profiles for Zagreb and Karlovac on 6 March 06 UTC, close to the time of strongest bora speed in the northern Adriatic (Jurčec, 1984, Bajić 1988). The bora layer was about 3 km deep, capped by the temperature inversions. The wind was rapidly weakening while turning from the bora NE direction to S-SSW. Due to stronger wind the Scorer parameter did not show such a pronounced maximum in the lower troposphere as it was the case in April. A characteristic feature is the profile of vertical acceleration with a low-level peak which is not generally seen on these profiles. What are the characteristics of the vertical profiles for the next day when the bora ceased in Omišalj but remained undisturbed in Senj, as seen in Fig. 1?

Fig. 2.7 shows that in Zagreb early in the morning of 7 March, during a rapid weakening of bora speed in Omišalj, the low troposphere was characterized by increased stability in a thicker layer. This feature was not so pronounced in terms of the Scorer parameter, since the wind speed was increasing in the low troposphere. The NE wind appears only in a very shallow layer close to the surface. At the end of this day, when Senj was still indicating strong bora, SW winds at the upper level increased, stability decreased and the temperature inversion was destroyed (Fig. 2.8). The low-level maxima of the Scorer parameter and vertical acceleration are no longer seen in the vertical profiles of these parameters.

Finally, Fig. 2.9 shows the characteristic profiles in Pula on 6 March at 12-hourly intervals. It is seen that the inversion was lowering and intensifying which together with wind weakening caused an increase of the Scorer parameter in the low troposphere.

Thus, weakening of low-tropospheric wind under stronger stability condition appears to be a common factor in both considered cases during bora weakening along the Adriatic coast. This, however, does not influence bora speed in Senj which is obviously influenced by another mechanism in agreement with Klemp and Durran's conclusion.

3. High Resolution Isentropic Time Cross-Sections

Figs. 3.1 - 3.3 show the vertical time cross-sections of the thermal field in terms of isentropes, for Zagreb, Pula and Zadar on 14 and 15 April 1982. The construction of these cross-sections is given in more detail in a recent paper by Glasnović (1990).

The low-tropospheric inversion layers followed in Fig. 2 are clearly seen on these cross-sections. A strong inversion is persistent in Zagreb at about an altitude of 3 km on the first day, and it lowers on the next day when two inversion layers appear in the afternoon.

Two inversions between 2 and 4 km are seen in Pula already on 14 April and the lowest appears close to the ground. It can be noticed that one of the higher level inversions is lowering and the other is rising, like in Zagreb.

In Zadar, the surface inversion is deeper on the first day and it is also rising in the afternoon when a higher level inversion forms. However, they are weaker in comparison to those in Pula, especially on the second day.

These cross-sections therefore show the inversion splitting and lowering, as already observed by aerial analysis (Smith, 1987), but they also indicate that the upstream thermal structure on 15th (the day of aircraft measurements) in the lower troposphere was not stationary on this day, as the theory requires.

4. Calculation of Hydraulic Parameters from the Specified Bora Layer Depth

In a previous paper (Glasnović and Jurčec, 1990) we have shown several cases of application of Smith's (1985) hydraulic theory. Starting with the basic characteristics of flow (U and N) the theory predicts the height of level H_0 which the fluid presumably selects as an origin of critical streamlines splitting over the mountain with the lower branch descending rapidly. The

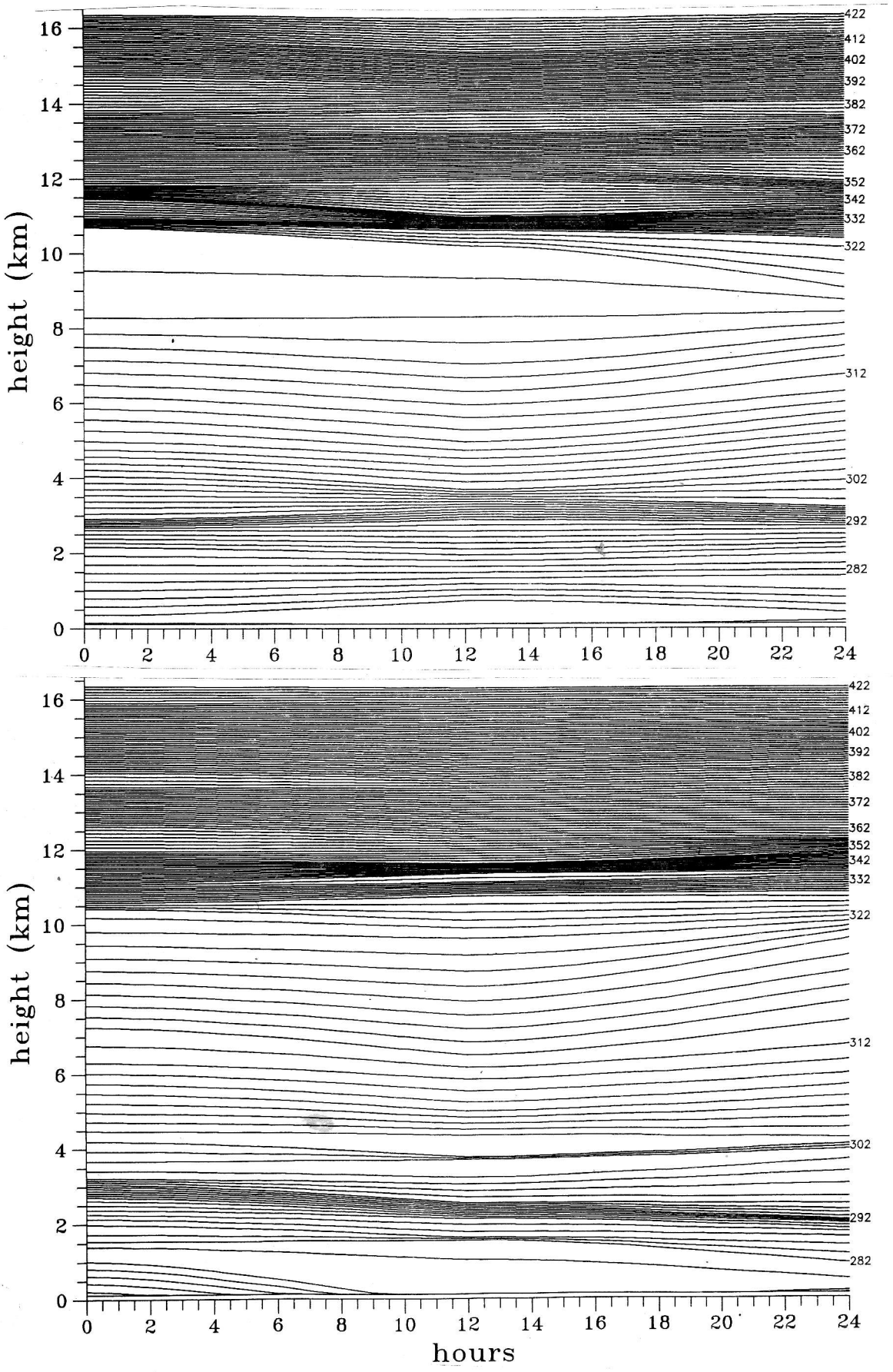

Fig. 3 Isentropic high resolution time cross-sections, 14 (above) - 15 (below) April 1982. 00 UTC + 24 /Analysis

Sl. 3 Izentropski vremenski vertikalni presjeci velike rezolucije, 14 (gore) - 15 (dolje) travanj 1982. 00 UTC + 24 /analiza

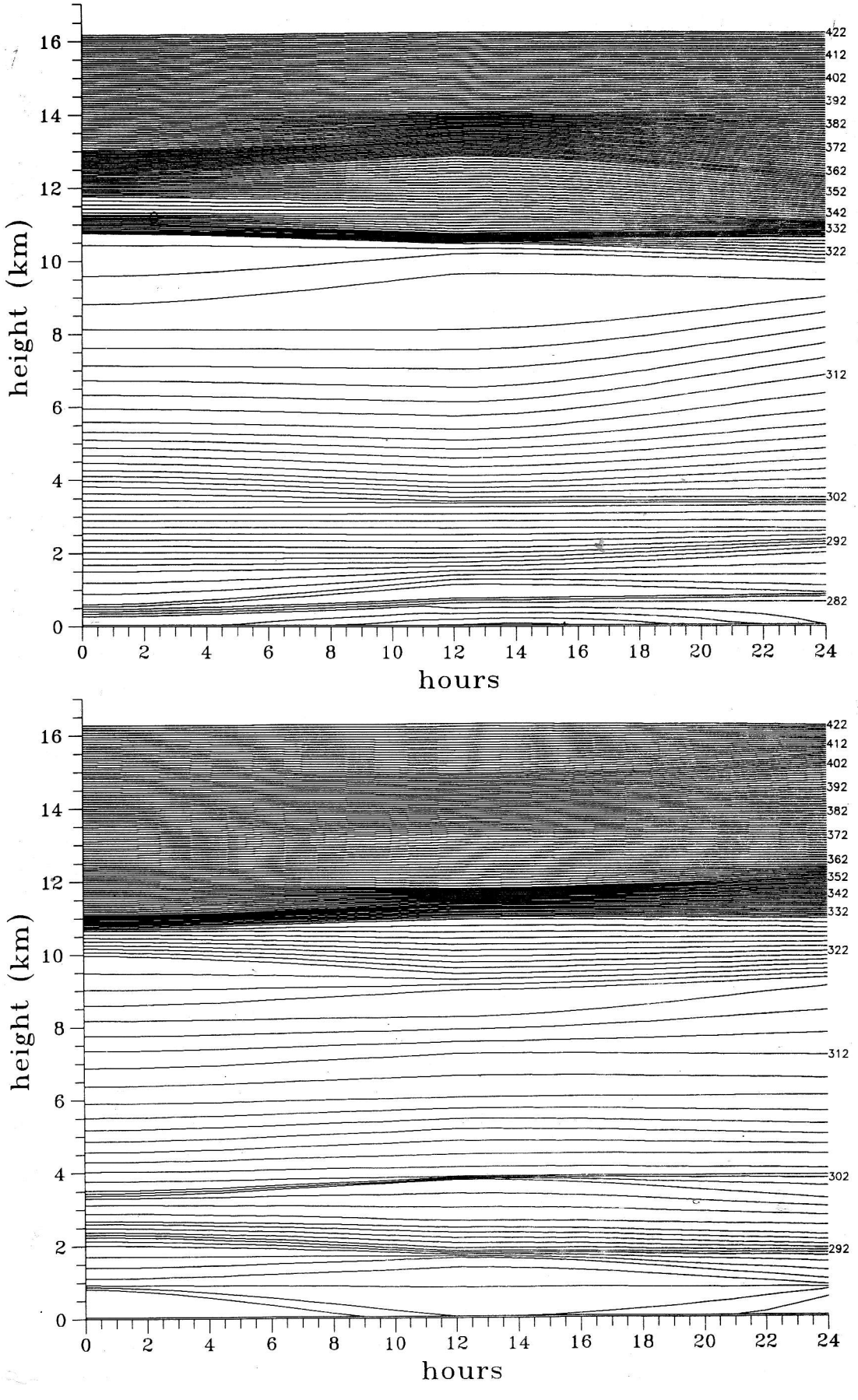

Fig. 3.2 Pula
Sl. 3.2 Pula

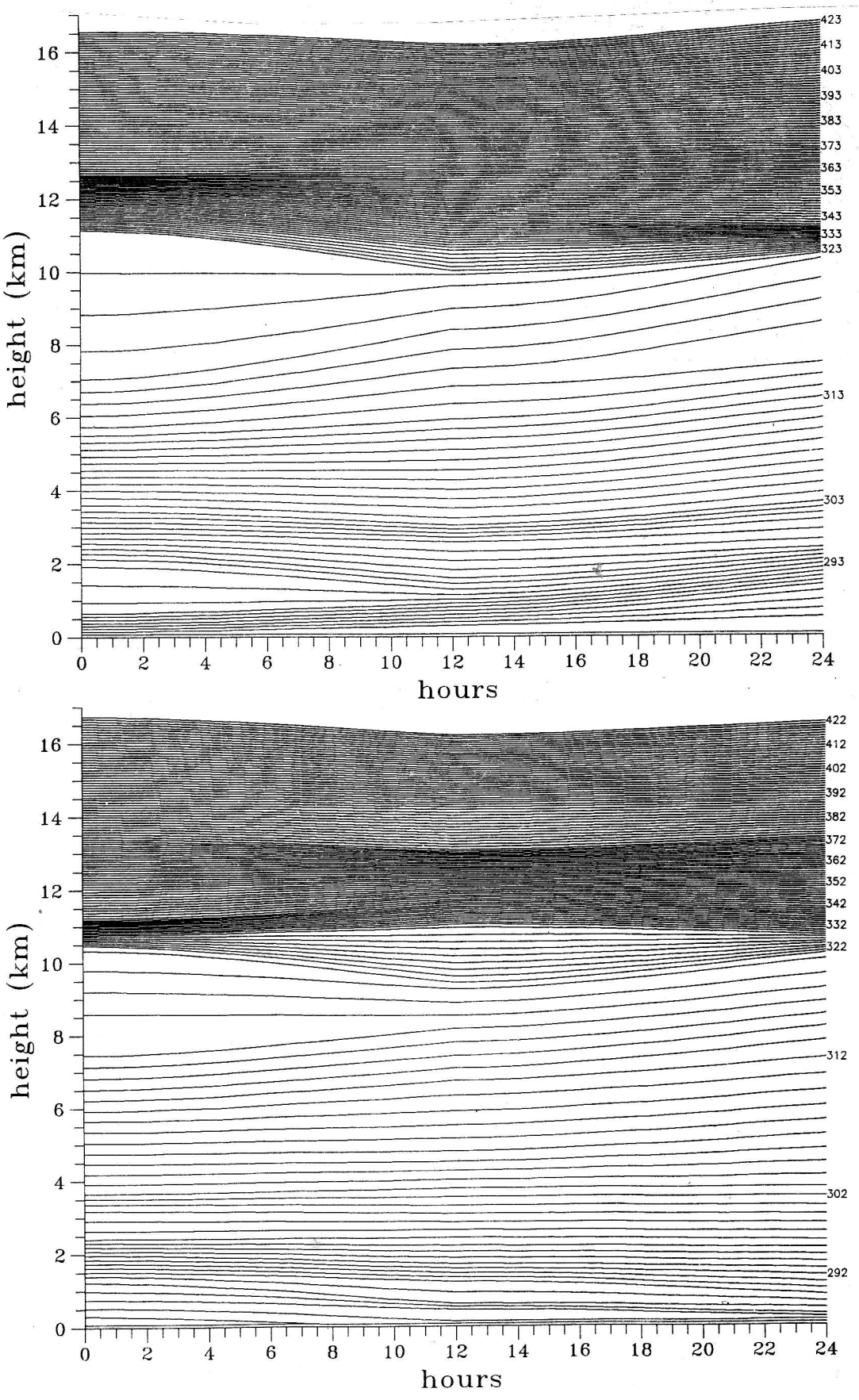

Fig. 3.3 Zadar
Sl. 3.3 Zadar

mountain height, h, is specified and in most bora reseach it is taken to be 800 m as used by Smith (1987). With such a procedure the analysis of extremely severe Adriatic bora storms shows (Jurčec, 1990) that only about 15% of cases satisfy Smith's criterion that $\hat{h} = h\ N/U < 1.0$. Thus, the question arises whether the mountain height could be lower in which case the theory could satisfy more real bora cases.

This paper presents more axamples of theory application where, with a defined H_0 and known fluid characteristics in terms of N and U, we calculate the corresponding h and the vertical displacement of the lower streamline δ from

$$\hat{h} = \hat{\delta}_c \cos(\hat{H}_0 + \hat{\delta}_c - \hat{h}) \qquad (6)$$

This relation is solved numerically by successive approximation to find $\hat{h}$ and the maximum mountain height h_m.

We have used several definitions for the bora layer height, H_0:

Class I. Wind direction is between 0 - 90° (as in Yoshino, 1976).

Class II. Only the "bora wind component" $U_b = 45 \pm 90°$, perpendicular to the mountain chain direction, is considered.

Class III. The bora layer is capped by the maximum of Scorer parameter, indicating stability inversion and/or minimum wind velocity. Under this definition only hydrostatic stability is considered inside the bora layer, whereas in the other three classes both hydrostatic (Tab. 1) and nonhydrostatic stability (Tab. 2) are considered.

Class IV. The bora layer is capped by the inversion expressed by the Brunt-Väisälä frequency profile. This corresponds to a single layer model, but it could also be applied to the model of continuous stratification as shown by Smith (1987) for 6 March.

The above objective determination of the bora layer height from empirical data is very sensitive to the upstream wind and temperature profiles, which could be influenced locally in the low-tropospheric layer and therefore may not be representative of the upstream bora condition. In this respect the period of ALPEX SOP is unique since two sounding stations, Zagreb and Karlovac, were available during the intensive observation period when the bora was being observed in the northern Adriatic.

Tab. 1. shows the "hydrostatic" hydraulic parameters for selected observations in the two cases considered, 6-7 March and 14-15 April. It is seen that the estimations of H_0, N_0 and U_0 are rather close in both stations and therefore the results are in general agreement. Since hydrostatic stability does not vary much, as already shown in section 2, the variations come mainly from the wind profiles. However, with the complex stability structure indicating several inversion layers in the low troposphere, in spite of small differences in both stations (as seen for example for 6 March in Fig. 2.5 and 2.6), the strongest inversion layer dictates the bora depth. In this particular case of 6 March, 06 UTC, the lowest inversion in Zagreb, which does not appear in Karlovac, is weaker and both stations have H_0 close to 2.6 km. Here, the iteration procedure gives a low $\hat{h}$, indicating no wave breaking. If in this case we take h = 800 m both stations have $\hat{h}$ close to 1.0. This would give a theoretical value, at 00 and 06 UTC, of H_0 = 3700 m close to the observed bora depth for class II and III. This means that h = 800 m is a good choice for mountain height in bora depth determination.

On the next day, when the northeasterly wind component extended to the lower stratosphere and the low-tropospheric inversion was not pronounced, the results of $\hat{h}_m$ and h_m received by the iteration procedure indicate larger differences. In particular, class II results in a very large $\hat{h}_8$ and a small h_m as the result of a dramatically decreased U_0 due to the influence of wind turning with height.

The choice of h = 800 m has not proved very successful in the second case study. On 14 April, during the strongest bora, the differences in the results between classes and between the two places become larger and on 15 April the iteration procedure does not offer acceptable results. Al-

Tab. 1 Hydraulic parameters for hydrostatic state, Zagreb and Karlovac.
Class I: wind direction 0 - 90°, Class II: U_b- component, Class III: Scorer parameter inversion, Class IV: temperature inversion (for further explanation see text).
Symbols: H_0 observed bora layer height according to defined classes, $\hat{H}_0$ nondimensional (=H_0 N/U), U_0 wind speed inside the bora layer, N_0 stability (Brunt-Väisälä frequency), L_z (=$2\pi/\ell$) vertical wave length, h_m mountain height calculated by iteration procedure (Eq. 6) and corresponding effective mountain height $\hat{h}_m$, and $\hat{h}_8$ for h = 800 m.

Tab. 1 Hidraulički parametri za hidrostatsko stanje, Zagreb i Karlovac.
Grupa I: smjer vjetra 0 - 90°, Grupa II: U_b - komponenta, Grupa III: Inverzija Scorerovog parametra, Grupa IV: inverzija temperature (za detaljnija objašnjenja vidi tekst na str.
Simboli: H_0. Opažena visina sloja bure prema definiranoj grupi. $\hat{H}_0$ (=H_0 N/U) bezdimenzionalna visina sloja bure, U_0 brzina vjetra unutar sloja bure, N_0 stabilnost (Brunt Väisälä frekvencija), L_z (=$2\pi/\ell$) vertikalna valna dužina, h_m visina planine izračunata iteracijom (relacija 6) i odgovarajuća efektivna visina planine $\hat{h}_m$, $\hat{h}_8$ efektivna visina za h = 800 m.

Month		ZAGREB								KARLOVAC							
Day	UTC	H_0 m	$\hat{H}_0$	U_0 ms^{-1}	N_0 10^{-2} s^{-1}	L_z	h_m m	$\hat{h}_m$	$\hat{h}_8$	H_0 m	$\hat{H}_0$	U_0 ms^{-1}	N_0 10^{-2} s^{-1}	L_z	h_m m	$\hat{h}_m$	$\hat{h}_8$
6.03.	00																
	I	2895	3.5	15.4	1.89	5128	408	0.50	0.98	3069	3.4	17.1	1.89	5668	402	0.45	0.89
	II	3757	5.6	12.8	1.90	4253	921	1.36	1.18	4015	5.4	14.2	1.90	4710	957	1.24	1.07
	III	3672	4.8	14.4	1.89	4795	785	1.03	1.05	3930	4.4	16.8	1.90	5560	767	0.87	0.90
	IV	2567	3.1	15.7	1.88	5230	275	0.33	0.96	2669	3.0	16.9	1.89	5618	265	0.30	0.89
6.03.	06																
	I	2958	3.8	14.8	1.89	4910	464	0.59	1.02	2941	3.5	16.0	1.90	5308	402	0.48	0.95
	II	3803	6.1	11.9	1.90	3934	1005	1.60	1.28	3913	5.6	13.2	1.91	4364	972	1.40	1.15
	III	3591	4.8	14.2	1.90	4702	765	1.02	1.07	3913	4.7	15.9	1.91	5256	811	0.97	0.96
	IV	2925	3.7	14.8	1.89	4923	449	0.57	1.02	2843	3.4	16.0	1.90	5293	367	0.44	0.95
7.03.	06																
	I	1019	1.8	10.9	1.88	3646	5	0.01	1.38	1629	2.8	10.8	1.88	3622	1.41	0.24	1.39
	II	13216	54.2	4.9	2.00	1531	162	0.66	3.28	13039	46.7	5.6	2.00	1756	55	0.20	2.86
	III	13616	17.5	15.6	2.00	4882	849	1.09	1.03	13603	16.2	16.8	2.00	5257	466	0.56	0.96
	IV	12076	14.3	16.9	1.99	5313	3	0.00	0.95	11929	13.0	18.3	1.99	5760	-	-	0.87
14.04.	12																
	I	1491	2.5	11.3	1.88	3777	86	0.14	1.33	2067	2.8	13.9	1.88	4647	174	0.24	1.08
	II	2428	5.8	7.9	1.88	2629	619	1.48	1.91	3311	6.5	9.6	1.89	3204	-	-	1.57
	III	2752	5.3	9.9	1.89	3278	645	1.24	1.53	3132	4.8	12.2	1.89	4073	672	1.04	1.23
	IV	1038	1.8	11.1	1.87	3715	4	0.01	1.35	3571	5.7	11.8	1.89	3938	896	1.43	1.28
15.04.	00																
	I	2254	5.8	7.3	1.88	2440	574	1.48	2,06	1917	5.3	6.9	1.88	2294	447	1.22	2.19
	II	2828	8.6	6.2	1.89	2059	36	0.11	2.44	2885	10.1	5.4	1.89	1802	169	0.59	2.79
	III	2708	7.2	7.1	1.89	2376	-	-	2.12	3038	8.2	7.0	1.89	2342	7	0.02	2.15
	IV	2945	8.0	7.0	1.89	2320	1	0.00	2.17	3038	8.2	7.0	1.89	2342	7	0.02	2.15
15.04.	12																
	I	1639	7.2	4.3	1.87	1431	-	-	3.51	1336	5.2	4.8	1.86	1629	306	1.18	3.09
	II	2239	12.9	3.2	1.87	1090	-	-	4.61	2339	12.2	3.6	1.87	1206	292	1.52	4.17
	III	2139	9.2	4.4	1.87	1464	62	0.27	3.34	2449	8.5	5.4	1.87	1803	25	0.09	2.79
	IV	1601	7.1	4.2	1.87	1422	-	-	3.53	2394	8.3	5.4	1.87	1803	14	0.05	2.79

Tab. 2 Nonhydrostatic hydraulic parameters. Classes and symbols as in Tab. 1

Tab. 2 Nehidrostatski hidraulički parametri. Grupe i simboli su kao u Tab. 1.

Tab. 2.1 ZAGREB

	H_o m	$\hat{H}_o$	U_o ms^{-1}	N 10^{-2} s^{-1}	L_z m	h_m m	$\hat{h}_m$	$\hat{h}_\theta$
6.03. 00								
I	2995	1.96	15.4	1.04	9268	48	0.03	0.54
II	3757	3.38	12.8	1.15	6983	486	0.44	0.72
III	3672	4.81	14.5	1.89	4795	784	1.03	1.05
IV	2567	1.56	15.7	0.95	10369	-	-	0.48
6.03. 06								
I	2958	2.07	14.8	1.04	8978	72	0.05	0.56
II	3803	3.78	11.9	1.18	6322	596	0.59	0.80
III	3591	4.80	14.2	1.90	4702	765	1.02	1.07
IV	2925	2.01	14.8	1.02	9161	57	0.04	0.55
7.03. 06								
I	1019	1.33	10.9	1.42	4822	-	-	1.04
II	13216	38.03	4.9	1.41	2173	-	-	2.31
III	13616	17.45	15.6	2.00	4882	849	1.09	1.03
IV	12076	9.78	16.8	1.36	7810	568	0.46	0.64
7.03. 12								
I	997	1.72	7.8	1.35	3637	3	0.00	1.38
II	11589	50.57	3.0	1.30	1439	-	-	3.49
III	13351	17.67	15.1	2.00	4748	874	1.16	1.06
IV	12169	10.44	16.0	1.38	7321	871	0.75	0.69
14.04. 00								
I	2156	4.29	6.4	1.26	3162	403	0.80	1.59
II	2495	5.84	5.7	1.32	2687	638	1.49	1.87
III	1012	4.76	4.0	1.87	1335	214	1.00	3.76
IV	2608	5.17	6.8	1.35	3169	600	1.19	1.56
14.04. 06								
I	2135	2.44	10.2	1.17	5503	116	0.13	0.91
II	2556	3.49	9.1	1.24	4604	350	0.48	1.09
III	2840	5.18	10.4	1.89	3445	653	1.19	1.46
IV	2840	3.50	10.4	1.28	5102	391	0.48	0.99
14.04. 12								
I	1491	1.78	11.3	1.35	5261	8	0.01	0.96
II	2428	4.32	7.9	1.40	3529	458	0.82	1.42
III	2752	5.27	9.9	1.89	3278	645	1.24	1.53
IV	1038	1.18	11.1	1.26	5515	-	-	0.91

Tab. 2.2 KARLOVAC

	H_o m	$\hat{H}_o$	U_o ms^{-1}	N 10^{-2} s^{-1}	L_z m	h_m m	$\hat{h}_m$	$\hat{h}_\theta$
6.03. 00								
I	3069	1.92	17.1	1.07	10059	41	0.03	0.50
II	4015	3.18	14.2	1.13	7941	459	0.36	0.63
III	3990	4.44	16.8	1.90	5560	766	0.87	0.90
IV	2669	1.56	16.9	0.99	10742	-	-	0.42
6.03. 06								
I	2941	2.10	16.0	1.15	8795	78	0.05	0.57
II	3913	3.74	13.2	1.26	6574	603	0.58	0.76
III	3913	4.68	15.9	1.91	5256	811	0.97	0.96
IV	2843	1.96	16.0	1.10	9132	45	0.03	0.55
7.03. 06								
I	1629	2.25	10.8	1.50	4538	63	0.09	1.11
II	13039	32.0	5.6	1.37	2559	-	-	1.96
III	13603	16.26	16.8	2.00	5257	466	0.56	0.96
IV	11929	8.72	18.3	1.34	8594	180	0.13	0.58
7.03. 18								
I	1801	3.84	7.5	1.60	2951	288	0.61	1.70
II	5673	16.90	4.3	1.28	2109	276	0.82	2.38
III	11620	14.03	16.5	1.99	5206	-	-	0.97
IV	11158	8.43	16.9	1.28	8314	86	0.07	0.60
6.03. 12								
I	3079	2.68	13.5	1.17	7227	229	0.20	0.70
II	5222	6.44	9.6	1.18	5097	-	-	0.99
III	2649	3.73	13.4	1.89	4464	406	0.57	1.13
IV	2128	1.68	13.1	1.01	7953	4	0.00	0.63
6.03. 18								
I	1999	1.37	15.1	1.03	9176	-	-	0.55
II	4860	6.90	8.9	1.27	4428	-	-	1.14
III	4860	5.36	17.3	1.91	5693	1157	1.28	0.88
IV	2990	2.27	17.0	1.29	8266	120	0.09	0.61
14.04. 18								
I	2735	5.24	7.2	1.38	3277	637	1.22	1.53
II	2852	6.03	6.6	1.40	2974	749	1.58	1.69
III	2852	7.48	7.2	1.89	2397	-	-	2.10
IV	2910	5.86	7.2	1.44	3119	747	1.51	1.61
15.04. 00								
I	2254	4.01	7.3	1.30	3536	385	0.68	1.42
II	2828	6.49	6.2	1.42	2737	-	-	1.84
III	2708	7.16	7.1	1.89	2376	-	-	2.12
IV	2945	6.17	7.0	1.46	2999	787	1.65	1.68
15.04. 06								
I	1753	4.08	4.5	1.05	2702	306	0.71	1.86
II	2454	8.91	3.5	1.28	1730	51	0.18	2.90
III	2577	10.11	4.8	1.89	1602	155	0.61	3.14
IV	2577	7.11	4.8	1.33	2276	-	-	2.21
15.04. 12								
I	1639	6.31	4.2	1.64	1634	-	-	3.08
II	2239	11.38	3.3	1.65	1236	228	1.16	4.07
III	2139	9.18	4.4	1.87	1464	62	0.27	3.43
IV	1601	6.12	4.2	1.62	1644	425	1.63	3.06
15.04. 18								
I	1803	2.56	5.2	1.42	4417	117	0.17	1.14
II	2307	6.07	4.1	1.07	2388	609	1.60	2.10
III	2395	8.61	5.2	1.87	1747	29	0.11	2.88
IV	2352	4.94	5.2	1.10	2990	516	1.09	1.68
14.04. 12								
I	2067	2.19	13.9	1.47	5931	69	0.07	0.85
II	3311	5.05	9.6	1.47	4119	744	1.13	1.22
III	3132	4.83	12.2	1.89	4073	671	1.04	1.23
IV	3571	4.54	11.8	1.50	4944	715	0.91	1.02
14.04. 18								
I	2775	3.39	12.0	1.47	5145	360	0.44	0.98
II	3132	4.72	10.2	1.54	4168	656	0.99	1.21
III	3289	5.51	11.3	1.68	3749	802	1.34	1.34
IV	2863	3.62	11.9	1.51	4964	418	0.53	1.01
15.04. 00								
I	1917	4.15	6.9	1.48	2905	343	0.74	1.73
II	2885	8.16	5.4	1.53	2222	7	0.02	2.15
III	3038	8.15	7.0	1.89	2342	7	0.02	2.15
IV	3038	6.84	7.0	1.58	2792	-	-	1.80
15.04. 12								
I	1336	2.51	4.8	0.91	3339	81	0.15	1.51
II	2339	8.34	3.6	1.28	1762	13	0.05	2.85
III	3038	8.15	7.0	1.89	2342	7	0.02	2.15
IV	3038	6.84	7.0	1.58	2791	-	-	1.80

though H_0 indicates smaller variations, U_0 is gradually weakening and the level of L_Z is lowering, frequently reaching altitudes below H_0.

Class III hydraulic parameters in Tab. 2.1 and 2.2 keep hydrostatic stability and therefore make possible comparison with the other nonhydrostatic classes. H_0 is determined in the same manner in both tables. A smaller N_0 for nonhydrostatic state causes a smaller $\hat{h}$ and a much larger L_Z. Due to a smaller $\hat{h}$ more cases satisfy Smith's criterion $\hat{h} < 1.0$ but at the same time this decreases the chance of wave breaking, as judged by this parameter. A generally higher L_Z gives more chance that $H_0 < L_Z$, but at the same time there are more cases in which the iteration procedure gives no solution due to the condition $H_0 < \pi/2$.

Figs. 4.1 - 4.3 show graphically some of the curves in the "positive mountain quadrant" ($\hat{h} > 0$, $\delta < 0$) according to Smith (1985).

Fig. 4.1 presents the curves for Zagreb on 6 March, under both hydrostatic and nonhydrostatic conditions. We have already seen (Tab. 2.2) that in a nonhydrostatic case class IV, at 00 UTC, has no solution in the positive mountain area. With a hydrostatic N_0 the curve in this class has the smallest $\hat{h}$ (Fig. 4.1 b). In particular, the class II curve has a large $\hat{h}$ which does not enter this quadrant at the zero-point. This is even more pronounced for the classes II curve at 06 UTC on this day (Fig. 4.1 c) with $\hat{h} = 1.60$ which belongs to the largest $\hat{h}_m$ values obtained by the iteration procedure.

Such extremes of $\hat{h}_m$ are also found on 15 April, 00 UTC (Fig. 4.2) and 12 UTC (Tab. 2.1), in Zagreb for class IV, whereas in Karlovac class IV at these times gives no solution (Fig. 4.3). The solution curves for Karlovac on 6 March, 06 UTC, and 14 April, 18 UTC (Fig. 4.3 a, b), show that maximum $\hat{h}_m$ is reached by the hydrostatic class III and in both cases the calculated mountain height h_m (Tab. 2.2) is approximately 800 m.

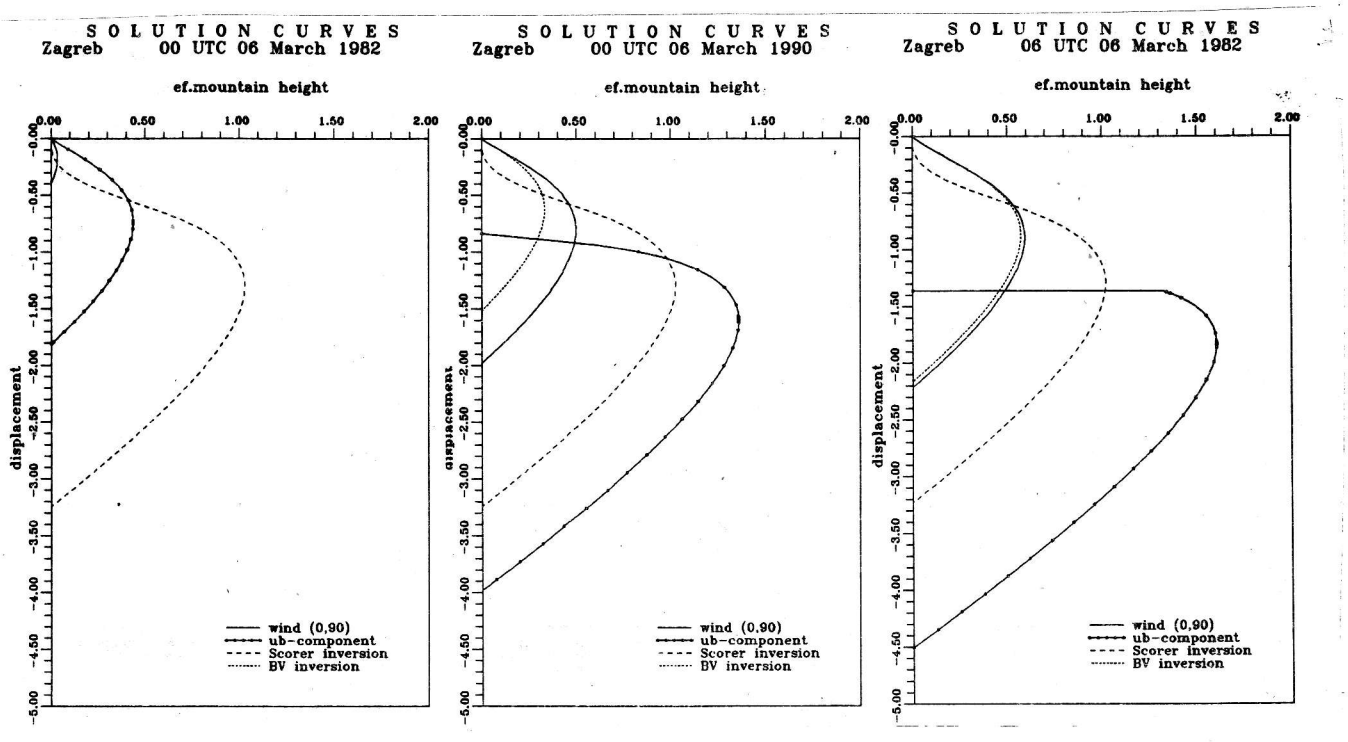

Fig. 4 Solution curves obtained by the iteration procedure (Eq. 6) in a positive mountain quadrant ($\hat{h} > 0$, $\hat{\delta} < 0$)
Sl. 4 Krivulje rješenja dobivene iteracijom (jedn. 6) u kvadrantu pozitivne planine ($\hat{h} > 0$, $\hat{\delta} < 0$)

Fig. 4.1 Zagreb, 6 March 00 UTC nonhydrostatic (a) and hydrostatic (b), 06 UTC hydrostatic (c).
Sl. 4.1 Zagreb, 6 ožujak 00 UTC nehidrostatski (a) i hidrostatski (b), 06 UTC hidrostatski (c).

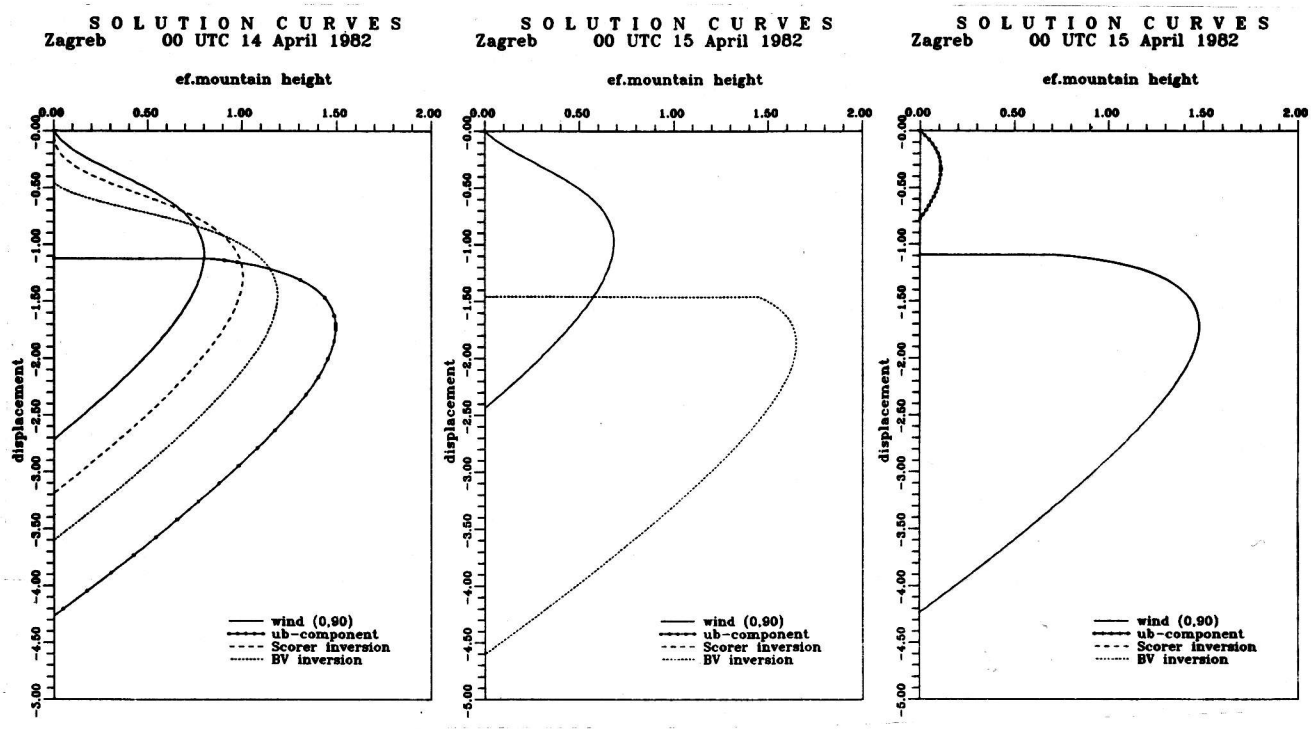

Fig. 4.2 Zagreb, 14 April 00 UTC nonhydrostatic (a), 15 April 00 UTC nonhydrostatic (b), and 15 April 00 UTC hydrostatic (c).

Sl. 4.2 Zagreb, 14 travanj 00 UTC nehidrostatski (a), 15 travanj 00 UTC nehidrostatski (b), i 15 travanj 00 UTC hidrostatski (c).

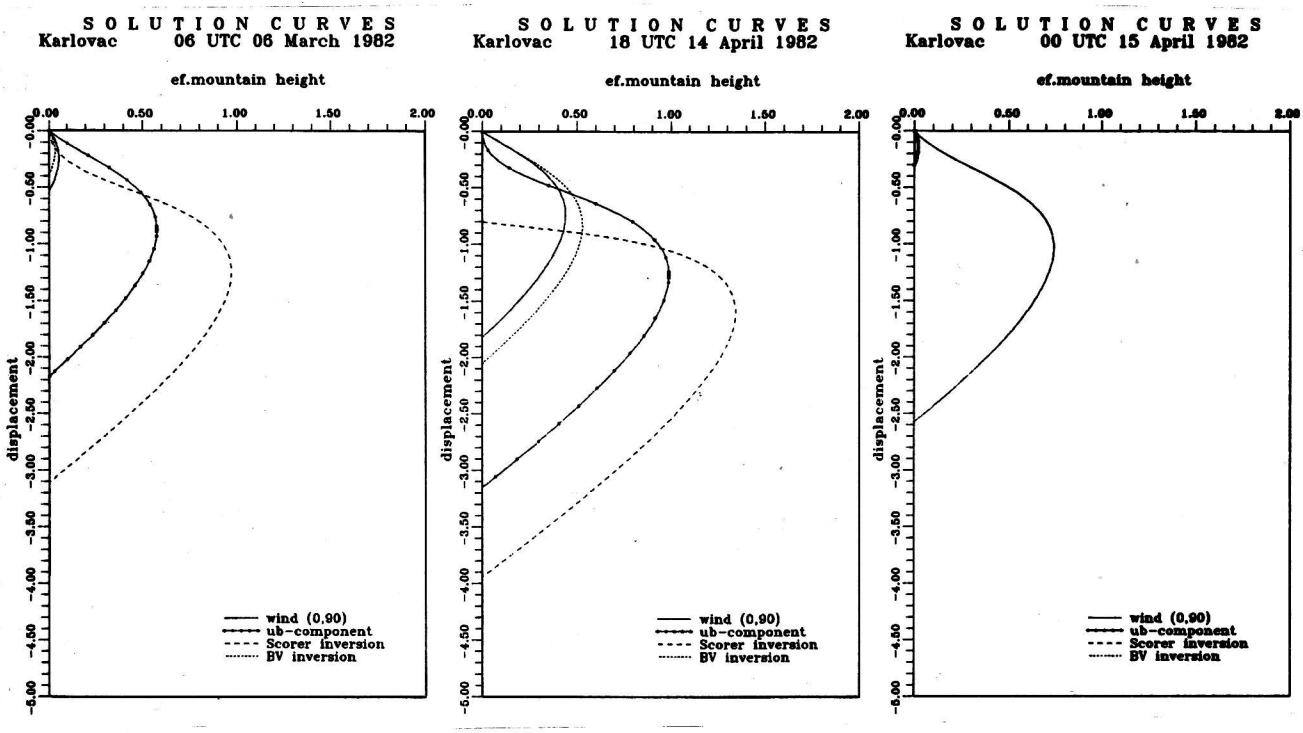

Fig. 4.3 Karlovac, 6 March 06 UTC nonhydrostatic (a), 14 April 18 UTC nonhydrostatic (b), 15 April 00 UTC nonhydrostatic (c).

Sl. 4.3 Karlovac, 6 ožujak 06 UTC nehidrostatski (a), 14 travanj 18 UTC nehidrostatski (b), 15 travanj 00 UTC nehidrostatski (c).

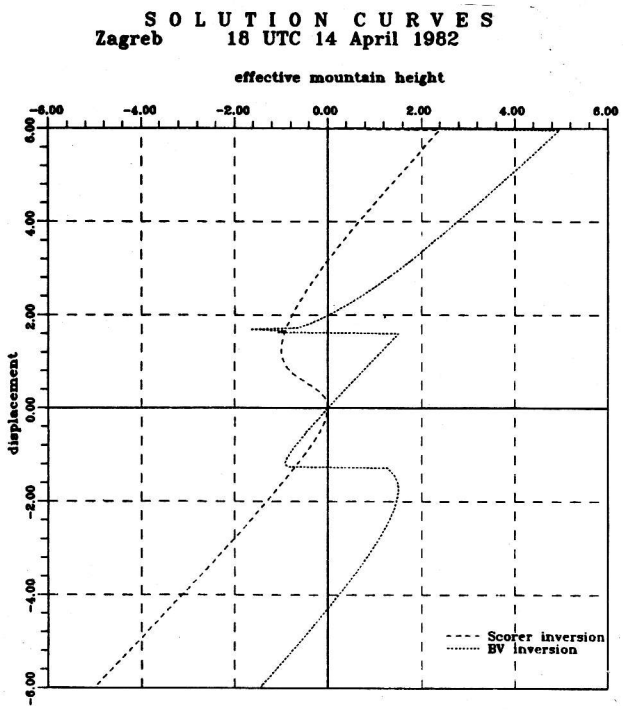

Fig. 5.1 14 April, 18 UTC
Sl. 5.1 14 travanj 18 UTC

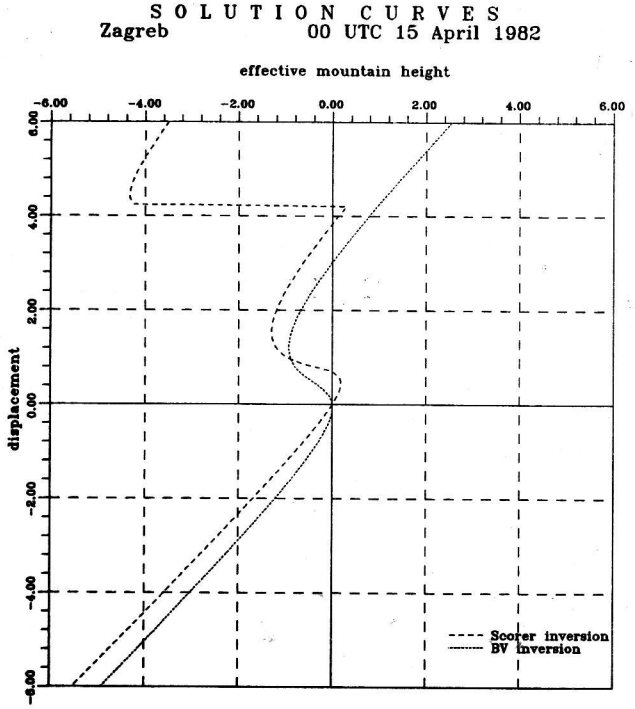

Fig. 5.2 15 April 00 UTC
Sl. 5.2 15 travanj 00 UTC

Fig. 5 Complete solution curves for Zagreb.
Sl. 5 Krivulje kompletnog rješenja za Zagreb

We can still not answer why these curves behave as they do and what the real meaning is of a h_m obtained by the iteration procedure. However, Fig. 5 gives a more complete picture of some curves which do not enter this area at the zero origin. Most of these curves indicate discontinuities outside the positive mountain area.

Fig. 5.1 on 14 April, 18 UTC, shows the curves of class III and IV. Class IV has a discontinuity at the negative δ-axis (close to $-\pi/2$) and therefore enters sharply the positive mountain area at this value of displacement. The class III curve does not appear in this quadrant. Fig. 5.2 shows two curves for 15 April, 00 UTC. These class III and IV curves in hydrostatic condition are also outside the positive mountain quadrant. For both curves $L_z < H_o$ as seen in Tab. 2.1.

These curves therefore indicate that in cases when bora occurs only in Senj the application of the hydraulic theory and the determination of bora depth and h_m from hydraulic parameters is questionable.

We believe that h_m which enters the iteration procedure does not represent the actual mountain height but it might be the part of this mountain above the upstream inversion layer. The inversion forms as a consequence of a blocking process, with cold stagnant air in the low-tropospheric layer. In such case the mountain shape should probably be considered, particularly the assymmetry which would result from such blocking. Therefore, for this and possible other processes, such as low-level splitting flow, instead of the 2-D hydraulic theory it is necessary to consider more complex three-dimensional flow through the mountain passes which are mostly responsible for local bora conditions.

5. Summary and Conclusions

The success of the application of Smith's internal hydraulic theory to some

real cases of Adriatic bora has finally encouraged a systematic study of the bora dynamics. At the same time, the theoretical approach to the bora as to a member of the severe downslope wind family, is essentially due to its very small scale, which can not be observed directly but only in interaction with a larger scale flow hopefully explanable by physical laws and mathematical tools.

This paper first stresses the well known fact that bora is a local phenomenon and that its longevity strongly depends on the local characteristics reacting to the mesoscale upstream bora flow in the low troposphere. This relationship is complex but we wish to study it through some simple models.

The low tropospheric structure presented by upstream temperature and wind profiles offers a qualitative picture of some bora flow characteristics. Although previous studies support an internal hydraulic mechanism for a strong bora case along the northern Adriatic coast, many questions are left open concerning the quantitative study and more details of this upstream flow structure. We have shown (Fig. 2, Tab. 1 and 2) that in many cases observational data do not clearly indicate bora depth and that various criteria, usually used for such a definition lead to different heights H_0 and consequently to different values of wind speed (U_0) and stability (N_0), inside a so defined bora layer, which are not constant as the present theory requires.

In order to calculate the theoretical value of H_0 we must know $\hat{h}$ including a selected mountain height h. Applying an opposite procedure instead of $\hat{h}$ we have defined H_0 and calculated the corresponding h from relation (6). It is shown that the usually accepted value h = 800 m appears in some classes, particularly in a hydrostatic state of stronger bora, but generally $\hat{h}$ and h show large variations among the different classes for the same day. In the particular case of 15 April, for which we have the results of the numerical simulation by Klemp and Durran (1987), we found great variations in $\hat{h}$ and for the various classes and the observations of both stations there is no solution for the curves in the positive mountain area, as defined by Smith (1985). For some cases this is illustrated in Fig. 4, while Fig. 5 shows complete solutions in all four quadrants. There is no clear physical explanation of such behaviour of the curves. We believe that the upstream blocking process in most postfrontal cases, when the bora occurs only in Senj, represents the main problem in the proper determination of mountain height from a known H_0. The observed slow wind U_0 resulted in a decrease of vertical wave length L_Z. A very large $\hat{h}_8$ (h = 800 m) would lead to wave breaking in agreement with the numerical simulation of bora for this case by Klemp and Durran. Although this process, or another mechanism associated with a cold air pool in the upstream area, was obviously responsible for the bora maintenance in Senj, we can not conclude that an inversion layer and changes in the upstream flow have no influence on bora speed at other localities, as illustrated by the bora decay in Omišalj in Fig. 1. A smaller speed of the bora component in all cases, and drastically pronounced on 7 March due to larger changes in wind direction, leads to the same conclusion. This clearly requires the consideration of a three-dimensional atmospheric structure in the final solution of the bora problem.

Acknowledgment: This research is based on the projects studies supported by the National Science Foundation of Croatia (No. 1-06-009) and the US-Yugoslav Joint Fund for Scientific and Technological Cooperation in cooperation with the NSF under Grant JF 990-0.

References

Bajić, A., 1988: The strongest bora event during ALPEX SOP. Rasprave-Papers, **23**, 1-12.

Clark, T.L. and W.R. Peltier, 1977: On the evolution and stability of finite amplitude mountain waves. J. Atmos. Sci., **34**, 1715-1730.

Durran, D.R. and J.B. Klemp, 1987: Another look at downslope winds. Part II: Nonlinear amplification beneath wave-overturning layers. J. Atmos. Sci., **44**, 3402-3412.

Glasnović, D., 1983: Dijagnostički izentropski model za istraživanje vertikalne strukture atmosfere (A diagnostic isentropic model for an investigation of the vertical atmospheric structure. In Croatian with English Summary). Hidrometeorološki zavod Hrvatske, Monografija, **1**, 33 str.

Glasnović, D.,1990: Isentropic high Resolution Time-Cross Section based on polynomial hydrostatic adjustment. Rasprave-Papers, **25**, 37-47.

Glasnović, D., and V. Jurčec, 1990: Determination of upstream bora layer depth. Meteorol. Atmos. Phys., **43**, 137-144.

Jurčec, V., 1990: Mountain drag and surface pressure variations during severe Adriatic bora storms. Rasprave-Papers, **25**, 25-36.

Jurčec, V., 1984: Strong bora case in Zadar and upstream bora layer characteristics. Zbornik meteoroloških i hidroloških radova, **10**, 105-108.

Klemp, J.B., and D.R. Durran, 1987: Numerical modeling of bora winds. Meteorol. Atmos. Phys., **36**, 215-227.

Peltier, W.R. and T.L. Clark, 1983: Nonlinear mountain waves in two and three spatial dimensions. Quart. J. Roy. Meteor. Soc., **109**, 527-548.

Smith, R.B., 1985: On severe downslope winds. J. Atmos. Sci., **42**, 2598-2603.

Smith, R.B., 1987: Aerial observations of the Yugoslavian bora. J. Atmos. Sci., **44**, 269-297.

Vučetić, V., 1988: Bora on the northern Adriatic, 12-18 April 1982. Rasprave-Papers, **23**, 27-44.

Kratak sadržaj

Iako je razvoj teorija zavjetrinskog vjetra, a posebno bure na Jadranu, nakon ALPEX-a konačno dobio važno mjesto u meteorološkim istraživanjima u nas i u svijetu, još uvijek nije utvrđen mehanizam olujne bure za veliki broj slučajeva. Posebno su malobrojne numeričke simulacije toka bure u navjetrini iz realnih podataka.

U ovom radu se posebno analizira slučaj bure od 15. travnja 1982. za koji postoje rezultati numeričke simulacije Klempa i Durrana, kojim se opovrgava važnost temperaturne inverzije i kritičnog nivoa (pri kojem isčezava komponenta bure, odnosno NE smjer vjetra na nekoj visini prelazi u suprotni SW smjer). Ovi autori naglašavaju da se njihovi rezultati odnose samo na promatranu specifičnu situaciju sa slabim vjetrom u navjetrini, uslijed čega dolazi do loma vala u vrlo niskoj troposferi ispod inverzije i kritičnog nivoa.

Uz analizu od 15. travnja prikazani su i rezultati za prethodni dan s jačom burom na mnogim stanicama sjevernog Jadrana, kao i slična situacija od 6-7. ožujka 1982. s najjačom burom u SOP. Na sl. 1 se ističe lokalni karakter bure u Senju uz perzistenciju vjetra u Senju u odnosu na obližnji Krk, gdje drugi dan bura slabi.

U poglavlju 2 dane su karakteristike vertikalnih profila temperature i vjetra, te izvedenih polja prikazanih na sl. 2 za Zagreb, Karlovac i Pulu. Pored karakteristične inverzije u donjoj troposferi uočava se da profil vjetra nije konstantan u sloju bure kako zahtjeva teorija, nego poprima oblik niske mlazne struje. Smanjenje vjetra uz povečanu stabilnost u sloju inverzije uzrokuje i izraziti maksimum u profilu Scorerovog parametra, koji je stoga uzet kao jedan od indikatora za objektivno određivanje visine sloja bure H_0 (Tab. 1 i 2).

Položaj inverzije u periodu 14-15. travanj za Zagreb, Pulu i Zadar na izentropskom vremenskom vertikalnom presjeku (sl. 3) jasno pokazuje promjene visine inverzije u ovoj "kvazi-stacionarnoj" situaciji.

U poglavlju 4 se prikazuju rezultati objektivnog određivanja visine sloja bure, H_0, valnog broja, L_Z, i efektivne visine, $\hat{h}_m$, određene relacijom (5) metodom iteracije, u usporedbi s efektivnom visinom $\hat{h}_8$, dobivenom za fiksnu vrijednost visine planine od 800 m uzetu u većini dosadašnjih radova koji koriste internu hidrauličku teoriju Smitha (npr. Smith, 1987, Jurčec, 1990). Upadljiv je plitki sloj bure uz slabljenje vjetra i smanjenje vertikalne valne dužine L_Z na dan 15.4. u odnosu na jaču buru prethodnog dana, a naročito oluju od 6.3. 1982.

Navedene karakteristike za 15.4. zajedno s visokim vrijednostima $\hat{h}$ prikazali su u svojim zaključcima na osnovi numeričke simulacije i Klemp i Durran (1987). Iz

usporedbe podataka Zagreba i Karlovca u tab. 1 za hidrostatsku stabilnost dobivenu relacijom (2) može se zaključiti da se osnovni hidraulički parametri u navjetrini bitno ne razlikuju. U ovim uvjetima visoke statičke stabilnosti je L_Z manja nego u nehidrostatskim uvjetima (Tab. 2). Ovi posljednji bi trebali prikazati realnije stanje atmosfere, iako se radi o srednjim vrijednostima stabilnosti i brzine vjetra u sloju bure, a ne o konstantnim vrijednostima kako to zahtjeva teorija. U tab. 2 vertikalna valna dužina pokazuje ekstremno visoke vrijednosti za vrijeme najjače bure 6. ožujka, iako postoje velike razlike među pojedinim grupama u kojima se H_0 ne razlikuje više od 1 km. Slijedećeg dana, 7.3., sve klase, izuzev I sa plitkim NE vjetrom, daju neprihvatljive vrijednosti sloja bure, ali se L_Z smanjuje i prema nekim kriterijima (klasama) došlo bi do loma vala na relativno niskim visinama gdje je i $\hat{h}$ velik. Međutim analiza (sl. 1) pokazuje da takav mehanizam ne podržava buru na sjevernom Jadranu, dok s druge strane lokalna bura u Senju ne reagira na ove promjene hidrauličkih parametara.

Konačno, odgovor na pitanje koja je optimalna visina prepreke h u primjeni hidrauličke teorije za "opažene" vrijednosti H_0 ne možemo dati, iako rezultati ukazuju da je u vrlo stabilnim uvjetima pri jakoj buri, kao što je bila 6.3. visina prepreke h = 800 m dosta dobra pretpostavka. Te vrijednosti i po prikazanim kriterijima klasa II - IV za određeni termin znatno variraju što dovodi u pitanje fizikalno značenje "visine planine" za ovako prikazane hidrauličke parametre. U mnogim slučajevima izračunati $\hat{h}$ i nemaju pozitivne vrijednosti. Matematički, to je u slučajevima $H_0 < \pi/2$ ili $H_0 > L_Z$, a grafički znači da krivulja ne pada u kvadrant "pozitivne" planine.

Nekoliko primjera grafikona za Zagreb i Karlovac koji padaju, sa sve četiri klase ili manje, u taj kvadrant prikazani su na sl. 4. Na primjer sl. 4.1 a) od 6.3. u 00 UTC pokazuje u skladu s vrijednostima $\hat{h}_m$ u tab. 2 tri krivulje sa sve većim $\hat{h}$ od I do III klase, dok klasa IV ne daje rješenje u tom kvadrantu ($H_0 < \pi/2$). U hidrostatskom slučaju sve četiri klase imaju rješenje i u dva uzastopna termina se bitno ne razlikuju, ali su veće razlike u istom terminu za Zagreb i Karlovac. Ovi rezultati pokazuju da je metoda jako osjetljiva na podatke o visini H_0, a time i vrijednosti stabilnosti i brzine vjetra unutar sloja bure ograničenog tom visinom. U mnogim slučajevima naročito za grupu IV određenu po inverziji temperature, krivulja ne prolazi ishodištem, odnosno ne ulazi direktno u pozitivni kvadrant iz ishodišta, a pored toga prelazi graničnu vrijednost $\hat{h} \leq 1.0$ prema teoriji Smitha. To se javlja za vrijeme olujne bure 6.3. u 06 UTC kao i 15.4. samo s lokalnom burom u Senju.

Da pokažemo da sve krivulje rješenja prema relaciji (5) prolaze kroz ishodište, ali ne moraju ući u pozitivni kvadrant, prilažemo sl. 5.1 - 5.3. Fizikalna interpretacija ovih krivulja s kompletnim rješenjima nije jasna, kao ni utjecaj tro-dimenzionalne strukture atmosfere na ponašanje bure i navjetrinskog toka preko (i oko) planine, pa to ostaje da se pokaže u narednim istraživanjima.